SPACECRAFT FORMATION CONTROL: MANAGING LINE-OF-SIGHT DRIFT BASED ON THE DYNAMICS OF RELATIVE MOTION

Richard J. Luquette[1] and Robert M. Sanner[2]

[1]*Goddard Space Flight Center, Code 591, Greenbelt, Maryland 20771, U.S.A.*
[2]*Department of Aerospace Engineering, University of Maryland, College Park, Maryland 20742, U.S.A.*

ABSTRACT

In a quest to improve space-based observational capability, an increasing number of investigators are proposing missions with precision formation flying architectures. Typical missions include the Micro-Arcsecond X-ray Imaging Mission (MAXIM), Stellar Imager (SI), and the New Worlds Observer (NWO). Missions designed to explore targets in deep-space generally require holding a formation configuration fixed in inertial space during science observation. Analysis in this paper is specifically aimed at the NWO architecture, characterizing the natural drift of the line-of-sight and the separation range for two spacecraft operating in the vicinity of the Earth/Moon-Sun L_2 libration point. Analysis employs a linear form of the relative dynamics associated with an n-body gravity field. The study is designed to identify favorable observation directions, characterized by minimal line-of-sight drift, along the mission timeline.

NOMENCLATURE

$A(t)$	=	Dynamics matrix for linear form of equations of motion
r_*	=	Position vectors, subscripts depicted in figures
$u_{thrust,F}$	=	External control force applied to Follower spacecraft
$u_{thrust,L}$	=	External control force applied to Leader spacecraft
x	=	Position of Follower referenced to Leader position
${}^I v$	=	Superscript designating inertial (I) frame
μ_i	=	Gravitational parameter for i^{th} body of n-body system
$\|x\|$	=	The 2-norm of the vector x

1. INTRODUCTION

Precision formation flying characterizes missions requiring relative state maintenance to very tight tolerances. Consequently, precision formation flying missions typically include continuous control schemes. Many candidate precision formation flying architectures are derived for missions designed to explore targets in deep space. These missions may be characterized by inertially fixed formation configurations during science observation periods. Generally, control tolerances are relaxed during reconfiguration maneuvers. Typical missions include: the Micro-Arcsecond X-ray Imaging Mission (MAXIM) [1], Stellar Imager (SI) [2], and the New Worlds Observer (NWO) [3].

NWO is a survey mission designed to discover and explore potential earth-like planets that exist outside the solar system. The mission concept includes two spacecraft, a telescope and an occulter. The telescope is designed to observe a planetary system about a star. The occulter is designed to block light from the star allowing observation of much dimmer planetary bodies orbiting the star. The challenge is to maintain the occulter on the telescope/target star line-of-sight, and to a lesser degree maintain the required telescope/occulter separation. With this configuration performance of NWO is much more sensitive to drift of the occulter off the line-of-sight direction than drift along the inter-spacecraft range.

To elaborate, assume the telescope is properly aimed along the line of sight to the target star. Optical performance requires the telescope/occulter spacecraft line of sight be maintained within an angle of 5 milli-arcseconds at 70,000 kilometers, equivalent to maintaining the occulter position within a meter (approximate) of the telescope/target line of sight. In contrast allowable drift along the line of sight is on the order of 100 kilometers from the desired range. Clearly performance of the telescope/occulter is much more sensitive to drift normal to the telescope/target line of sight than along the line of sight, relative spacecraft range. This motivates a desire to align the natural drift between the two spacecraft along the separation vector, minimizing the line-of-sight drift. Previewing this paper, the approach exploits the linear form of the relative dynamics, identifying the eigen-

vectors for the dynamics matrix in the linear state equation. Minimal drift in the direction normal to the telescope/target line of sight is achieved by aligning the observation vector with an eigenvector of the matrix representing the linear form of the relative spacecraft dynamics. The eigenvectors evolve with the formation trajectory. Ideally with a target rich environment, a targeting strategy might constrain observations to lie along (near) a particular eigenvector. In practice this strategy severely limits mission planning and target selection. A better strategy weights relative spacecraft drift as one of the factors in designing the mission observation schedule.

True coalignment of an eigenvector and the line-of-sight is not achievable for the duration of a given observation. The linear form of the dynamics are time varying. The eigenvectors of the dynamics matrix slowly rotate in inertial space. The observation vector is fixed in inertial space.

While the analysis centers on the NWO mission, the development and results generically apply to any similar formation architecture.

2. RELATIVE DYNAMICS

As noted, the analysis goal is to identify the relative range vector orientations that minimize natural drift of the range vector direction. The natural relative dynamics for a spacecraft formation operating near the Earth/Moon-Sun L_2 libration point are principally forced by differential gravity and solar pressure. The gravitational differential acceleration is a space environment characteristic, independent of spacecraft design. In contrast, differential acceleration due to solar pressure is a design consideration tightly correlated to the physical properties of the spacecraft, and subject to variation with the orientation of the spacecraft with respect to the incident solar radiation. This analysis is limited to characterizing the differential gravity field.

Reference [4] presents the development of the linear form for the relative dynamics in inertial coordinates for the restricted three body problem, depicted in Fig. 1. References [5] and [6] extend the development for the n-body problem, depicted in Fig. 2. The development of the linear form of the relative dynamics for the n-body problem is repeated in summary form for reference.

2.1. Dynamics of Relative Motion for the n-Body Problem

The n-body problem examines the behavior of an infinitesimal mass in the combined gravitational field of 'n' finite masses orbiting their common center of mass. A typical two spacecraft formation operates in the gravitational field of n-bodies, as shown in Fig. 2.

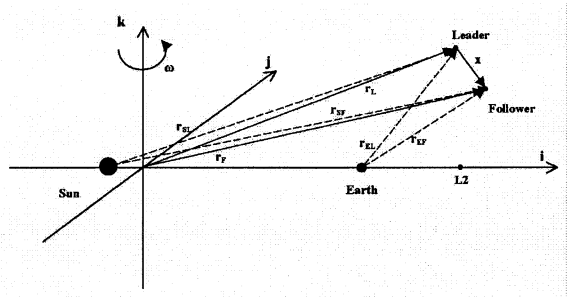

Figure 1. Two Spacecraft Orbiting in the Earth/Moon - Sun Rotating Frame

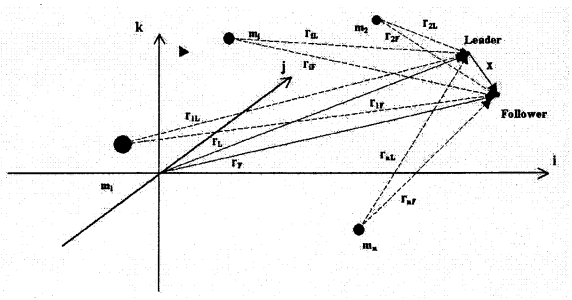

Figure 2. Two Spacecraft Under the Gravitational Influence of n-Bodies

Treating each body as a point mass and allowing spacecraft thrust, the equation of relative motion of the Follower with respect to the Leader is:

$$
\begin{aligned}
\ddot{\boldsymbol{x}} &= \ddot{\boldsymbol{r}}_F - \ddot{\boldsymbol{r}}_L \\
&= -\sum_{i=1}^{n} \mu_i \frac{\boldsymbol{r}_{iF}}{\|\boldsymbol{r}_{iF}\|^3} + \boldsymbol{u}_{thrust,F} \\
&\quad - \left(-\sum_{i=1}^{n} \mu_i \frac{\boldsymbol{r}_{iL}}{\|\boldsymbol{r}_{iL}\|^3} + \boldsymbol{u}_{thrust,L} \right) \\
&= (\boldsymbol{u}_{thrust,F} - \boldsymbol{u}_{thrust,L}) - \left\{ \sum_{i=1}^{n} \frac{\mu_i}{\|\boldsymbol{r}_{iF}\|^3} \right\} \boldsymbol{x} \\
&\quad - \sum_{i=1}^{n} \mu_i \left\{ \frac{1}{\|\boldsymbol{r}_{iF}\|^3} - \frac{1}{\|\boldsymbol{r}_{iL}\|^3} \right\} \boldsymbol{r}_{iL}
\end{aligned}
\tag{1}
$$

Eq. 1, presented for a gravity field in an inertial frame, provides an exact expression of the nonlinear dynamics of relative motion between the Follower and Leader spacecraft. The next step expresses the relative dynamics

of the Follower with respect to the Leader in linear form.

2.2. Linear Form of Relative Dynamics

Transforming Eq. 1 to a linear form requires examination of each term. Consider $\left\{\frac{1}{\|\boldsymbol{r}_{iF}\|^3} - \frac{1}{\|\boldsymbol{r}_{iL}\|^3}\right\}$

$$\begin{aligned}
&\left\{\frac{1}{\|\boldsymbol{r}_{iF}\|^3} - \frac{1}{\|\boldsymbol{r}_{iL}\|^3}\right\} \\
&= \left\{\frac{1}{\|\boldsymbol{r}_{iL} + \boldsymbol{x}\|^3} - \frac{1}{\|\boldsymbol{r}_{iL}\|^3}\right\} \\
&= \left\{\frac{1}{[(\boldsymbol{r}_{iL} + \boldsymbol{x})^{\mathsf{T}}(\boldsymbol{r}_{iL} + \boldsymbol{x})]^{3/2}} - \frac{1}{\|\boldsymbol{r}_{iL}\|^3}\right\} \\
&= \left\{\left[\|\boldsymbol{r}_{iL}\|^2 + \boldsymbol{x}^{\mathsf{T}}\boldsymbol{x} + 2\,(\boldsymbol{r}_{iL}{}^{\mathsf{T}}\boldsymbol{x})\right]^{-3/2} - \|\boldsymbol{r}_{iL}\|^{-3}\right\} \\
&= \left\{\left[1 + \frac{\boldsymbol{x}^{\mathsf{T}}\boldsymbol{x}}{\|\boldsymbol{r}_{iL}\|^2} + 2\,\frac{(\boldsymbol{r}_{iL}{}^{\mathsf{T}}\boldsymbol{x})}{\|\boldsymbol{r}_{iL}\|^2}\right]^{-3/2} - 1\right\}\|\boldsymbol{r}_{iL}\|^{-3}
\end{aligned} \tag{2}$$

Apply a binomial expansion to first order, resulting in

$$\begin{aligned}
&\left\{\frac{1}{\|\boldsymbol{r}_{iF}\|^3} - \frac{1}{\|\boldsymbol{r}_{iL}\|^3}\right\} \\
&= \left\{\left[1 + \frac{\boldsymbol{x}^{\mathsf{T}}\boldsymbol{x}}{\|\boldsymbol{r}_{iL}\|^2} + 2\,\frac{(\boldsymbol{r}_{iL}{}^{\mathsf{T}}\boldsymbol{x})}{\|\boldsymbol{r}_{iL}\|^2}\right]^{-3/2} - 1\right\}\|\boldsymbol{r}_{iL}\|^{-3} \\
&= \left\{\left[1 + (-\frac{3}{2})\left(\frac{\boldsymbol{x}^{\mathsf{T}}\boldsymbol{x}}{\|\boldsymbol{r}_{iL}\|^2} + 2\,\frac{(\boldsymbol{r}_{iL}{}^{\mathsf{T}}\boldsymbol{x})}{\|\boldsymbol{r}_{iL}\|^2}\right) + H.O.T.\right] \right. \\
&\qquad\qquad \left. - 1\right\}\|\boldsymbol{r}_{iL}\|^{-3} \\
&\approx -\frac{3}{2}\left(\frac{\boldsymbol{x}^{\mathsf{T}}\boldsymbol{x}}{\|\boldsymbol{r}_{iL}\|^2} + 2\,\frac{(\boldsymbol{r}_{iL}{}^{\mathsf{T}}\boldsymbol{x})}{\|\boldsymbol{r}_{iL}\|^2}\right)\|\boldsymbol{r}_{iL}\|^{-3}
\end{aligned} \tag{3}$$

It follows from Eq. 3 that

$$\sum_{i=1}^{n} \frac{\mu_i}{\|\boldsymbol{r}_{iF}\|^3} \tag{4}$$

$$\approx \sum_{i=1}^{n} \frac{\mu_i}{\|\boldsymbol{r}_{iL}\|^3}\left(1 - \frac{3}{2}\frac{\boldsymbol{x}^{\mathsf{T}}\boldsymbol{x}}{\|\boldsymbol{r}_{iL}\|^2} - 3\,\frac{(\boldsymbol{r}_{iL}{}^{\mathsf{T}}\boldsymbol{x})}{\|\boldsymbol{r}_{iL}\|^2}\right)$$

Substituting Eqs. 3 and 4 into Eq. 1 gives

$$\begin{aligned}
\ddot{\boldsymbol{x}} \approx &-\left\{\sum_{i=1}^{n}\frac{\mu_i}{\|\boldsymbol{r}_{iL}\|^3}\left(1 - \frac{3}{2}\frac{\boldsymbol{x}^{\mathsf{T}}\boldsymbol{x}}{\|\boldsymbol{r}_{iL}\|^2} \right.\right. \\
&\qquad \left.\left. - 3\,\frac{(\boldsymbol{r}_{iL}{}^{\mathsf{T}}\boldsymbol{x})}{\|\boldsymbol{r}_{iL}\|^2}\right)\right\}\boldsymbol{x} \\
&+ \sum_{i=1}^{n}\left\{\frac{\mu_i}{\|\boldsymbol{r}_{iL}\|^5}\left(\frac{3}{2}\boldsymbol{x}^{\mathsf{T}}\boldsymbol{x} + 3\,\boldsymbol{r}_{iL}{}^{\mathsf{T}}\boldsymbol{x}\right)\boldsymbol{r}_{iL}\right\} \\
&+ (\boldsymbol{u}_{thrust,F} - \boldsymbol{u}_{thrust,L})
\end{aligned} \tag{5}$$

Replace $(\boldsymbol{x}^{\mathsf{T}}\boldsymbol{x})\ \boldsymbol{r}_{iL}$ and $(\boldsymbol{r}_{iL}{}^{\mathsf{T}}\boldsymbol{x})\ \boldsymbol{r}_{iL}$ in Eq. 5 with the equivalent expressions, $(\boldsymbol{r}_{iL}\ \boldsymbol{x}^{\mathsf{T}})\ \boldsymbol{x}$ and $(\boldsymbol{r}_{iL}\ \boldsymbol{r}_{iL}{}^{\mathsf{T}})\ \boldsymbol{x}$, yielding

$$\begin{aligned}
\ddot{\boldsymbol{x}} &\approx -\left\{\sum_{i=1}^{n}\frac{\mu_i}{\|\boldsymbol{r}_{iL}\|^3}\left(1 - \frac{3}{2}\frac{\boldsymbol{x}^{\mathsf{T}}\boldsymbol{x}}{\|\boldsymbol{r}_{iL}\|^2} - 3\,\frac{(\boldsymbol{r}_{iL}{}^{\mathsf{T}}\boldsymbol{x})}{\|\boldsymbol{r}_{iL}\|^2}\right)\right\}\boldsymbol{x} \\
&\quad + \sum_{i=1}^{n}\left\{\frac{\mu_i}{\|\boldsymbol{r}_{iL}\|^5}\left(\frac{3}{2}\boldsymbol{r}_{iL}\,\boldsymbol{x}^{\mathsf{T}} + 3\,\boldsymbol{r}_{iL}\,\boldsymbol{r}_{iL}{}^{\mathsf{T}}\right)\boldsymbol{x}\right\} \\
&\quad + (\boldsymbol{u}_{thrust,F} - \boldsymbol{u}_{thrust,L}) \\
&= -\left\{\sum_{i=1}^{n}\frac{\mu_i}{\|\boldsymbol{r}_{iL}\|^3}\left[\left(1 - \frac{3}{2}\frac{\boldsymbol{x}^{\mathsf{T}}\boldsymbol{x}}{\|\boldsymbol{r}_{iL}\|^2} - 3\,\frac{(\boldsymbol{r}_{iL}{}^{\mathsf{T}}\boldsymbol{x})}{\|\boldsymbol{r}_{iL}\|^2}\right)\mathbf{I_3}\right.\right. \\
&\qquad \left.\left. + \frac{1}{\|\boldsymbol{r}_{iL}\|^2}\left(\frac{3}{2}\boldsymbol{r}_{iL}\,\boldsymbol{x}^{\mathsf{T}} + 3\,\boldsymbol{r}_{iL}\,\boldsymbol{r}_{iL}{}^{\mathsf{T}}\right)\right]\right\}\boldsymbol{x} \\
&\quad + (\boldsymbol{u}_{thrust,F} - \boldsymbol{u}_{thrust,L})
\end{aligned} \tag{6}$$

In order to remove the state dependence of the dynamics matrix in Eq. 6, assume a tight formation with $\|\boldsymbol{x}\| << \|\boldsymbol{r}_{iL}\|$, for all i. Thus, $\left\|-\frac{3}{2}\frac{\boldsymbol{x}^{\mathsf{T}}\boldsymbol{x}}{\|\boldsymbol{r}_{iL}\|^2} - 3\,\frac{(\boldsymbol{r}_{iL}{}^{\mathsf{T}}\boldsymbol{x})}{\|\boldsymbol{r}_{iL}\|^2}\right\| << 1$. Likewise, the term $\frac{3}{2}\frac{\boldsymbol{r}_{iL}\,\boldsymbol{x}^{\mathsf{T}}}{\|\boldsymbol{r}_{iL}\|^2}$ is also neglected, since its matrix norm is much smaller than the remaining terms. Eq. 6 simplifies to

$$\begin{aligned}
\ddot{\boldsymbol{x}} &= -\left\{\sum_{i=1}^{n}\frac{\mu_i}{\|\boldsymbol{r}_{iL}\|^3}\left[\mathbf{I_3} \right.\right. \\
&\qquad \left.\left. + \frac{3}{\|\boldsymbol{r}_{iL}\|^2}(\,\boldsymbol{r}_{iL}\,\boldsymbol{r}_{iL}{}^{\mathsf{T}})\right]\right\}\boldsymbol{x} \\
&\quad + (\boldsymbol{u}_{thrust,F} - \boldsymbol{u}_{thrust,L}) \\
&= -\left\{\sum_{i=1}^{n}\frac{\mu_i}{\|\boldsymbol{r}_{iL}\|^3}\left[\mathbf{I_3} + 3(\,\boldsymbol{e}_{iL}\,\boldsymbol{e}_{iL}{}^{\mathsf{T}})\right]\right\}\boldsymbol{x} \\
&\quad + (\boldsymbol{u}_{thrust,F} - \boldsymbol{u}_{thrust,L})
\end{aligned} \tag{7}$$

Note that $\boldsymbol{e}_{iL}$ denotes a unit vector along $\boldsymbol{r}_{iL}$.

In summary the linear form of the dynamics is expressed as

$$\ddot{x} \;\; = {}^{I}\Xi(t)\; x + u_{thrust,F} - u_{thrust,L} \qquad (8)$$

where

$${}^{I}\Xi(t) \;\; = -\sum_{i=1}^{n} \frac{\mu_i}{\|r_{iL}\|^3} \left[\mathbf{I_3} \; + \; 3(\, e_{iL}\; e_{iL}{}^{\mathsf{T}})\right]$$

The dynamics in matrix form are

$$\dot{\xi} \;\; = {}^{I}A(t)\; \xi \; + B\; (u_{thrust,F} - u_{thrust,L}) \qquad (9)$$

Where:

$$\xi = \begin{bmatrix} x \\ \dot{x} \end{bmatrix}; \quad {}^{I}A(t) = \begin{bmatrix} \mathbf{0} & \mathbf{I_3} \\ {}^{I}\Xi(t) & \mathbf{0} \end{bmatrix}; \quad B = \begin{bmatrix} \mathbf{0} \\ \mathbf{I_3} \end{bmatrix}$$

2.3. Characterizing Relative Drift

Based on the previous discussion, the term ${}^{I}\Xi(t)$ characterizes the gravity gradient between the two spacecraft. ${}^{I}\Xi(t)$ provides a linear form of the relative acceleration, referenced to the leader spacecraft. ${}^{I}\Xi(t)$ is time varying with a very slow evolution correlated with the nominal 6-month period for an orbit about the Earth/Moon-Sun L_2 point. Using the NWO mission concept, the science schedule generally limits the total time for each individual target to two days with less than a day of actual science observation time. Consequently, the relative spacecraft dynamics for a single observation can be characterized by a nominal, constant ${}^{I}\Xi(t)$.

Following the assumption ${}^{I}\Xi(t)$ is constant, the magnitude and direction of the relative spacecraft acceleration is defined by the eigenvalues and associated eigenvectors of ${}^{I}\Xi(t_0)$. t_0 represents the nominal point in time for the science observation. Referring to Eq. 8, ${}^{I}\Xi(t)$ is symmetric. Therefore, the eigenvectors are mutually perpendicular. The orientation of the eigenvectors is approximated by evaluating ${}^{I}\Xi(t_0)$ with only the contributions of Sun and Earth/Moon system gravity fields, expressed as:

$$\begin{aligned} {}^{I}\Xi(t_0) \;\; &= \{-(c_1 + c_2)\; \mathbf{I_3} \\ &\quad +3\; c_1\; [e_{EL}(t_0)\; e_{EL}(t_0)^{\mathsf{T}}] \\ &\quad +3\; c_2\; [e_{SL}(t_0)\; e_{SL}(t_0)^{\mathsf{T}}] \\ c_1 \;\; &= \mu_{em} \|r_{EL}\|^{-3} \\ c_2 \;\; &= \mu_s \|r_{SL}\|^{-3} \end{aligned} \qquad (10)$$

Where $e_{SL}(t_0)$ and $e_{EL}(t_0)$ represent unit vectors from the Sun to the Leader, and the Earth/Moon mass center to the Leader, respectively. By inspection one eigenvector is a unit vector in the direction of the cross product of $e_{SL}(t_0)$ and $e_{EL}(t_0)$ with an eigenvalue of $-(c_1 + c_2)$. The two remaining eigenvectors lie in the plane spanned by $e_{SL}(t_0)$ and $e_{EL}(t_0)$. The special case with $e_{SL}(t_0)$ and $e_{EL}(t_0)$ collinear is not considered since the configuration is not achievable along expected trajectories for a mission near the Earth/Moon-Sun L_2point. The typical orientation of the eigenvectors is depicted in Fig. 3. For an orbit about the Earth/Moon-Sun L_2 point the eigenvalue associated with e_2 is positive, representing an unstable mode. The eigenvalues of e_1 and e_3 are negative, representing stable modes. Stability properties are for the nominal ${}^{I}\Xi(t_0)$.

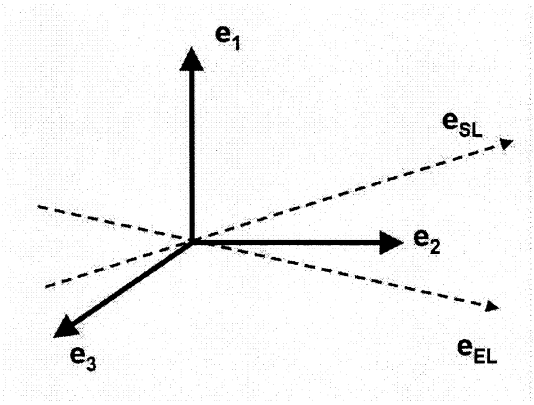

Figure 3. Orientation of Eigenvectors (e_1, e_2, e_3) of ${}^{I}\Xi(t_0)$ relative to $e_{SL}(t_0)$ and $e_{EL}(t_0)$

Alignment of the formation along any of the eigenvector directions restricts the relative spacecraft (gravitational) acceleration along the separation vector. Following the eigenvector designations from Fig. 3, the e_1 direction generally aligns nearly with the spacecraft to Sun line, a direction typically prohibited for science observations by deep-space exploration mission constraints. Therefore, e_2 and e_3 are the allowable, principal observing directions that minimize angular drift of the line-of-sight.

3. SIMULATION

Simulation results demonstrate the variation in the radial and crosstrack line of sight drift along a representative trajectory for the NWO mission. The observation vector is fixed in inertial space with a spacecraft separation range of 72,000 kilometers. The nominal orbit for the telescope spacecraft about the Earth/Moon-Sun L_2 point is shown in Fig. 4.

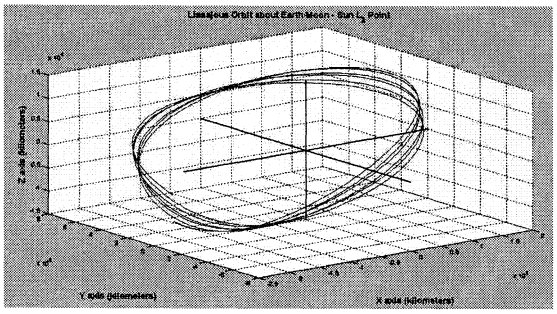

Figure 4. Leader (Telescope) Spacecraft Trajectory about Earth/Moon-Sun L_2 point

3.1. Scenario 1 – Observation Vector Normal to Ecliptic Plane

In the first scenario the observation vector is defined to align with the normal direction for the ecliptic plane. Fig. 5 shows the relative acceleration between the two spacecraft with respect to the mission timeline. The principal component of the relative acceleration remains aligned with the observation (range) vector along the entire orbit.

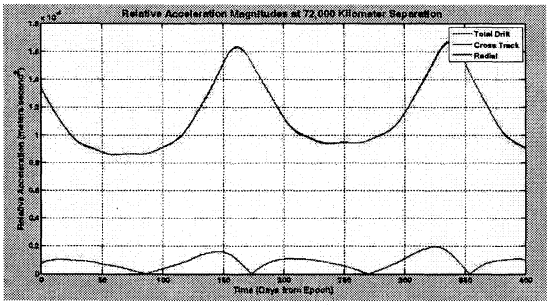

Figure 5. Relative Acceleration of Follower with Respect to Leader for Observation Vector Normal to Ecliptic Plane

3.2. Scenario 2 – Observation Vector within Ecliptic Plane

In the second scenario the observation vector is defined to lie within the ecliptic plane. The observation vector is initially aligned with the Earth/Sun line. Fig. 6 shows the relative acceleration between the two spacecraft with respect to the mission timeline. The components of the relative acceleration exhibit significant variation along the mission timeline. Fig. 7 depicts the same results as a function of the angle between the observation vector and the eigenvector for the unstable mode of ${}^{I}\Xi(t)$. The unstable mode is the e_2 direction shown in Fig. 3. The results indicate the crosstrack drift is minimum for observation vectors along the unstable mode eigenvector of ${}^{I}\Xi(t_0)$, or perpendicular to that vector. The results apply to a vector confined to the ecliptic plane. NWO mission science constraints prohibit observations along the unstable mode eigenvector, e_2, since it nominally aligns with the spacecraft to Sun vector.

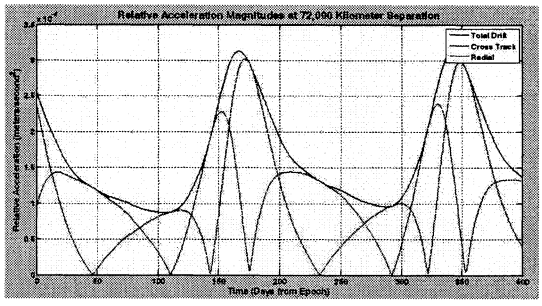

Figure 6. Relative Acceleration of Follower with Respect to Leader for Observation Vector within the Ecliptic Plane as a Function of Mission Timeline

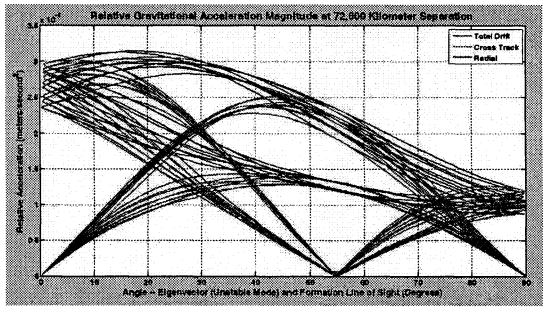

Figure 7. Relative Acceleration of Follower with Respect to Leader for Observation Vector within the Ecliptic Plane as a Function of Angular Separation Between Observation Vector and eigenvector e_1 of ${}^{I}\Xi(t_0)$.

4. CONCLUSIONS

This work demonstrates the utility of employing the linearized relative dynamics for a spacecraft formation as a planning tool for scheduling observations. The linearized dynamic model identifies preferred observation directions which minimize natural drift of the formation line-of-sight. Preferred directions align with the eigenvectors of the matrix representation of the linear form of the dynamics. The strategy assumes the mission science goals are achievable with the imposed constraint on the observation line-of-sight.

REFERENCES

[1] "The Micro-Arcsecond X-ray Imaging Mission (MAXIM) Homepage," http://maxim.gsfc.nasa.gov/

[2] "The Stellar Imager (SI) Homepage," http://hires.gsfc.nasa.gov/si/

[3] "The New Worlds Observer (NWO) Homepage," http://newworlds.colorado.edu/

[4] Luquette, R. J. and Sanner, R. M., "Linear State-Space Representation of the Dynamics of Relative Motion, Based on Restricted Three Body Dynamics," *AIAA Guidance and Control Conference*, August 2004, Paper No. AIAA-2004-4783.

[5] Luquette, R. J. and Leitner, J. and Gendreau, K. C. and Sanner, R. M., "Formation Control for the MAXIM Mission," *2nd International Symposium on Formation Flying Mission & Technologies* , September 2004.

[6] Luquette, R. J., "Nonlinear Control Design Techniques for Precision Formation Flying at Lagrange Points," Ph.D. Dissertation, Department of Aerospace Engineering, University of Maryland, College Park, MD, December 2006.